數據解讀、海報製作、實例欣賞
(成果分享)

邏輯撰述、分享新知
(2016年09月)

Wen-Hsien Li (李文献)
中央大學 中子束應用研究中心
物理系 奈米物性實驗室
whli@phy.ncu.edu.tw

科展主軸議題

科展議題 -- 尋自然哲理

科學心境 -- 享自然之美

科學方法 -- 讓證據顯現

科學態度 -- 讓證據說話

科學分析 -- 循邏輯漸進

科學結論 -- 找簡單之理

心思心境

(追尋新奇、淡看認知)

whli@phy.ncu.edu.tw

蘋果箴言

To create something new,
you have to be disconnected
from your past.

捨棄認知、跳脫意識

迪卡兒箴言

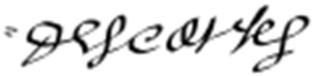

To attend the true in life we must discard all the ideals that we were taught and reconstruct the entire system of our knowledge.

我思故我在

René Descartes
法國，1596~1650

電影 The girl king: 瑞典克里斯蒂娜女王

1. 絕不承認任何事物為真，我完全不懷疑的事物才視為真理；
2. 將每個問題分成若干個簡單的部分來處理；
3. 思想必須從簡單到複雜；
4. 應該時常進行徹底的檢查，確保沒有遺漏任何東西。

視界

- “太陽下山” 與 “太陽下海”
- “旭日東昇” 與 “旭日南起”
- 顛覆才有創新

- **Experience and exploration outside textbooks**

心思

藉實驗數據思考、思考、再思考：

我可以看到什麼，

我可以問什麼問題；

我可以再作什麼，

我可以提出什麼見解。

放眼新知

別讓已知牽引你，

別讓已知框限你；

別俸認知為聖旨，

別為認知來瞎忙。

找尋已知之不知、撰述自然之未現

觀點

以數據的觀點看自然，

非以認知觀點看自然；

以自創的情節說自然，

非以認知情節套自然。

無需再證實已知

視界

無國界學校：
“動手做”是未來學習的關鍵字

- 提供感染科學方法與獨立思考的訓練。
- 藉由實作經驗來精進觀測技術。
- 藉由實驗發現來領悟知識。
- 藉由推理數據來理解並分享自然。
- 書本學習是累積別人的經驗，但不能被前人的經驗所局限。

化解認知的衝突

紅	橘	綠	紫	藍
藍	黑	紅	綠	橘
紫	黑	橘	紅	紫
黑	紅	橘	綠	紫
PU	BK	OR	RE	PU
BK	RE	OR	GE	PU

創意與科學

創意之源

- **Out-of-box thinking（靈活心思）**
- **Passion（熱忱態度）**
- **Critical thinking（核心之慮）**

科學之美

- **A journey to nature (自然之旅)**
- **A vision to future (未來之見)**

數據解讀

(歸納化繁瑣、慧眼識英雄)

whli@phy.ncu.edu.tw

以反應速率實驗為例

1.

3 ml water +
3 drops of HCl
= dilute HCl solution

2.

Add 2 drops of universal indicator.

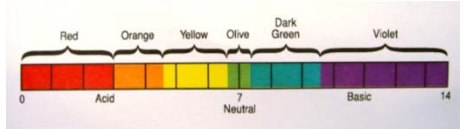

判斷PH值

3.

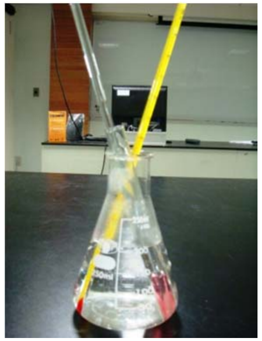

加熱後，紀錄熱平衡溫度

4.

加入1/4片錠制酸劑，並攪拌開始計時。

5.

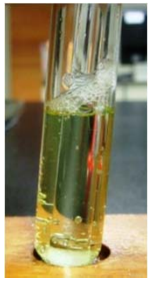

待溶液成中性，停止計時。

1. 選定HCl溶液濃度，紀錄反應時間與溫度之關係。
2. 改變HCl溶液濃度，討論溶液濃度對反應速率之影響。

數據解讀

境界:以簡易關係示連結物理量

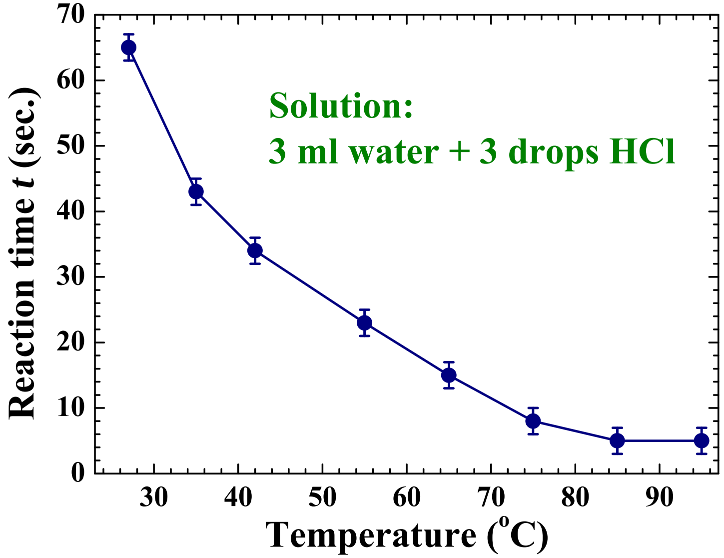

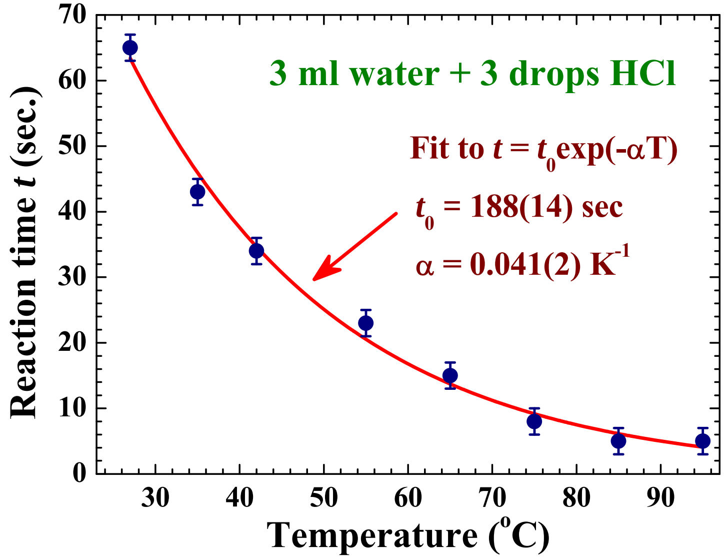

- 僅能說反應時間隨溫度升高而縮短。
- 能進而以一溫度係數來描述反應時間的縮短變率及主控機制。(溫度區間沒有新物理或化學作用發生)
- 誤差值指的是儀器精準度不能以多次平均取得。
- **3 drops: scientifically not precise enough.**

關係式判定

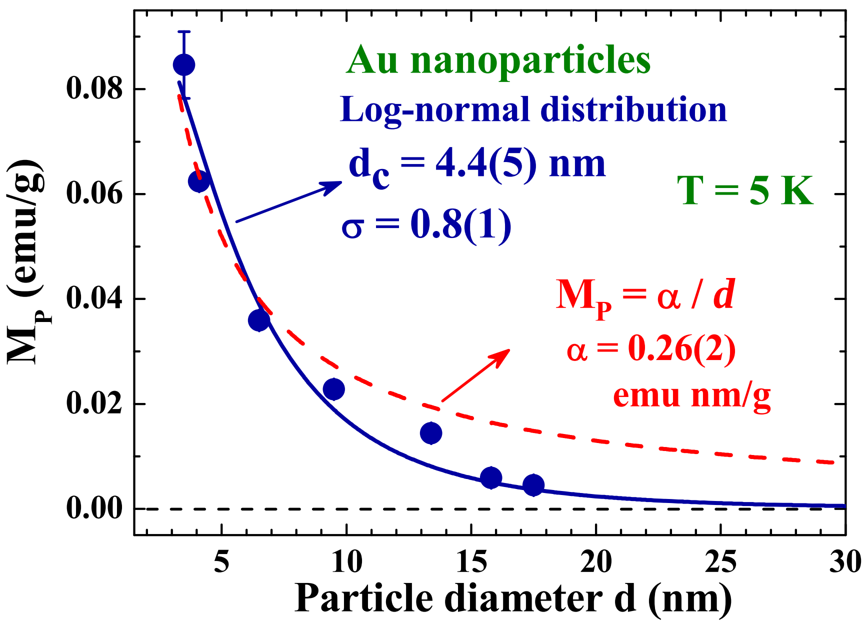

- 物理參數間的依附關係，提供物理運作機制的訊息。
- 以數據擬合來判定參數間的依附關係。

- 主軸議題：金奈米顆粒中具磁性的原子(僅表面原子?)
- 一次方反比關係難以完整描述金奈米顆粒的磁矩與粒徑間的關係，顯示表面原子並非是惟一提供磁性的原子。

實例欣賞

Studies of cell elasticity by nonlinear damping (2011, Intel 2nd Award)

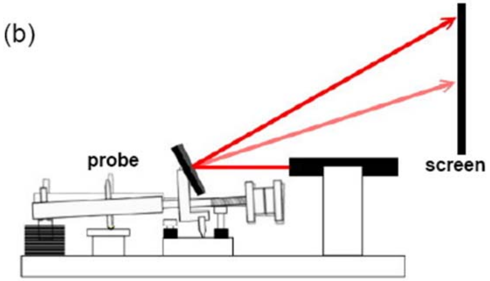

- 自製簡易磁動力光槓桿，記錄振盪曲線
- 光槓桿(放大微小型變)、磁動力(以磁力大小調變應力)
- 探針下放置軟物質，如斑馬魚卵，記錄光槓桿振盪曲線
- 如何理解振盪曲線所隱含的物理資訊
- 探針下壓：魚卵被壓縮，探討魚卵的抗拒能力(內部結構)
- 探針離開：魚卵黏滯探針，探討魚卵的黏滯力(表面特質)
- 探討孵化各週期、或各選定酸鹼環境下魚卵的彈力特質
- 需能描述非線性運動振盪
- 探針下壓時魚卵會滋生抗拒力保護自己

非線性擺動資訊萃取

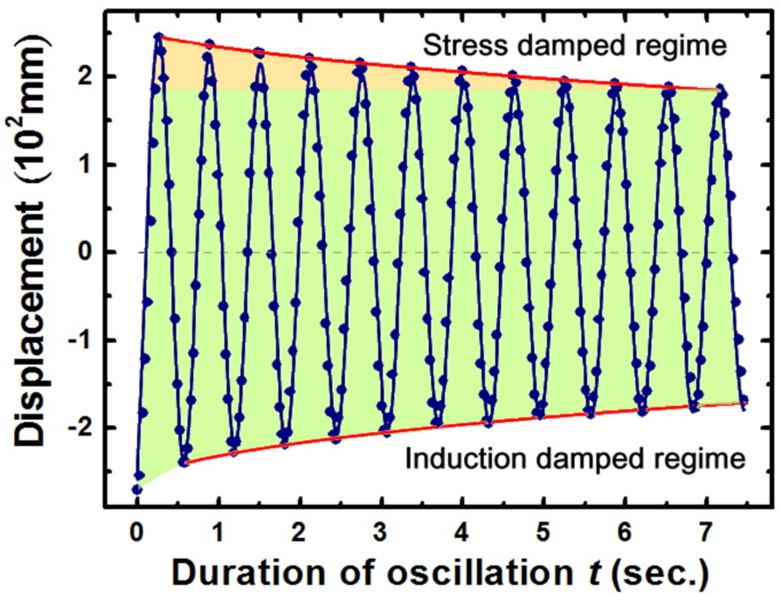

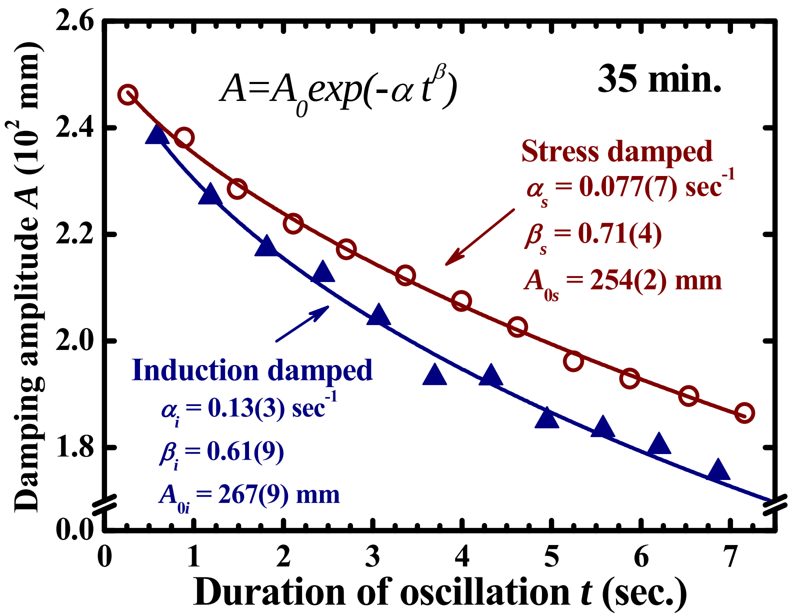

- 主軸議題：非彈性擺幅認定
- 區分成接觸魚卵(stress damped)與脫離魚卵(induction damped)區域。
- 槓桿下壓與離開魚卵時擺幅的衰退(damping)程度各異，以衰退係數談論魚卵對承受外力與自我回復的反應。

實例欣賞

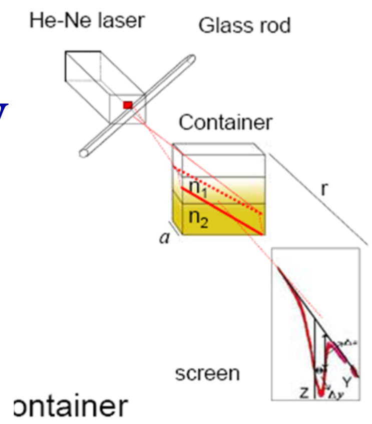

Nonlinear diffusion dynamics measured by simple light-transmission method (2010, Intel 3rd Award)

- 雷射筆光點通過玻璃棒 → 單色光線光源
- 一液體懸浮在另一液體上方 → 介面間兩液體相互擴散
- 單色光線光源通過介面區域，偵測透射光形狀，記錄透射光形狀隨時間的變化
- 光透射過介面被曲折的程度與介面的密度有關 → 推算出介面區域密度隨時間的改變量
- 量測出一液體擴散至另一液體的位能障值
- 303 K的熱能就能有效的破壞甘油間分子間的鍵能
- 甘油-水介面：初期，水與甘油間形成氫鍵引發擴散
  後期，水與甘油間密度的不同引發擴散

以光折射探討動態擴散

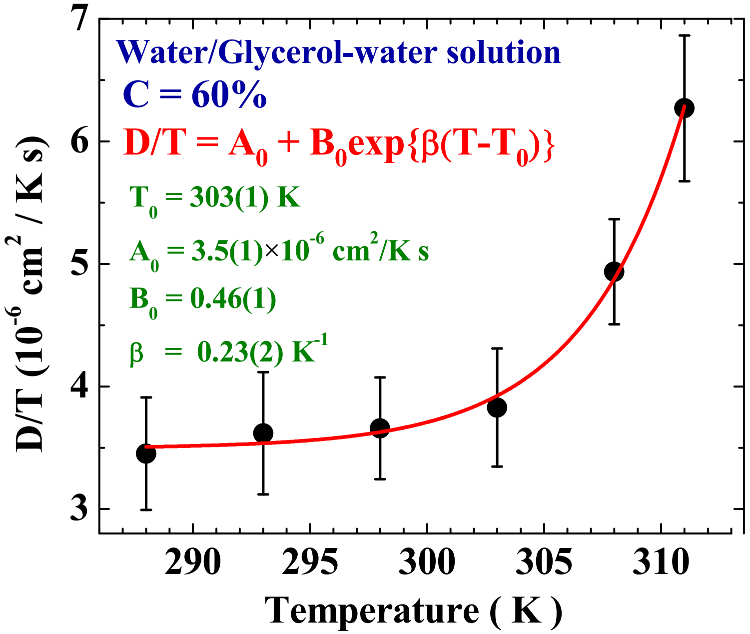

- 主軸議題：液態界面間的擴散係數在溫度高於300K時開始急遽上升的原因。
- 液態界面間的擴散係數與溫度的關係，可以用指數遞增函數來描述。

- 擴散係數急遽上升，因緣於甘油間分子鍵的熱鬆解，而允許甘油與水分子間形成氫鍵。
- 擬合所得溫度常數為303 K，顯示裂解甘油間分子鍵的能障為303 K = 26.1 meV。
- 相變區數據點仍嫌不足。

實例欣賞

Evuvuv – the air messager

(2007, Intel 2nd Award)

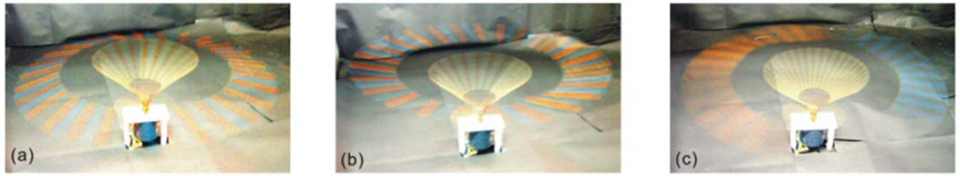

- 繩子拉接響片，接轉動馬達定速旋轉，記錄其運動軌跡
- 繩子：可扭轉、不可扭轉
- 響片：薄片、圓柱、半圓柱、三角柱、四方柱
- 僅薄片接於可扭轉繩子，才能發出聲響
- 響片在袱角與仰角間連續轉換，響聲頻率也隨之改變
- 觀測到三旋轉態：繩子順時針方向扭轉、不扭轉、逆時針方向扭轉
- 響片自繩子接收能量與釋放能量給繩子的時間週期不同。
- 聲音來源：Evuvuv 自轉時拍打空氣

動態能量轉移

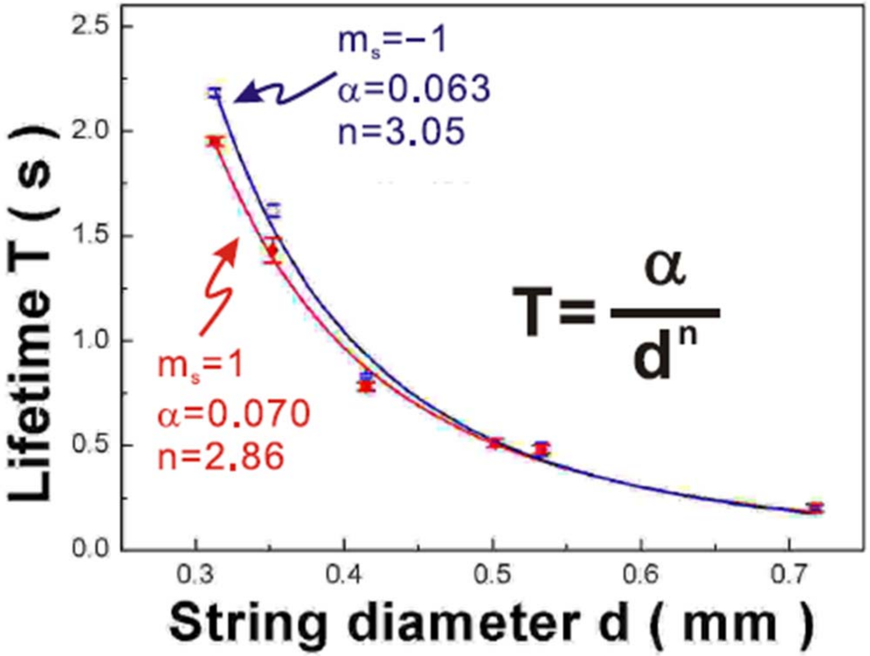

- 主軸議題：繩子與響片間能量的轉移。
- 靜態時，扭轉繩子所需能量與繩子直徑的4次方成正比。
- $m_s = -1$: 響片接收能量
  $m_s = 1$: 響片釋放能量

- 響片轉動週期隨繩子直徑的3.05 (接收能量)或2.86 (釋放能量)次方變動，顯示響片與繩子間的能量轉移牽涉動態機制。
- 可進一步探討動態能量。

圖示魅力

圖一幅更勝字一百
畫龍需點睛，意境得點醒

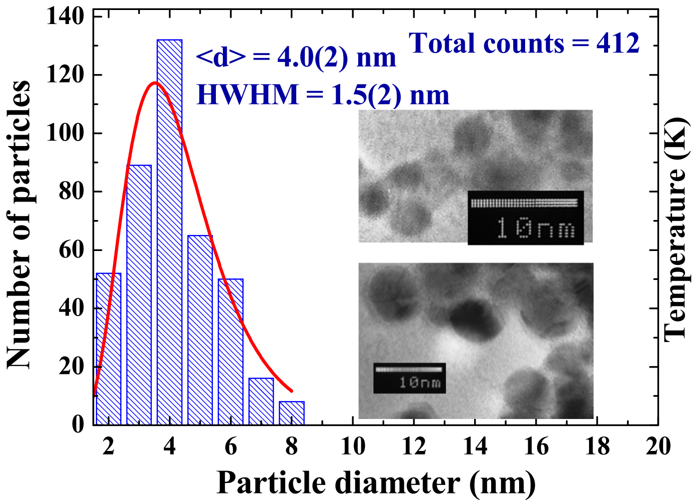

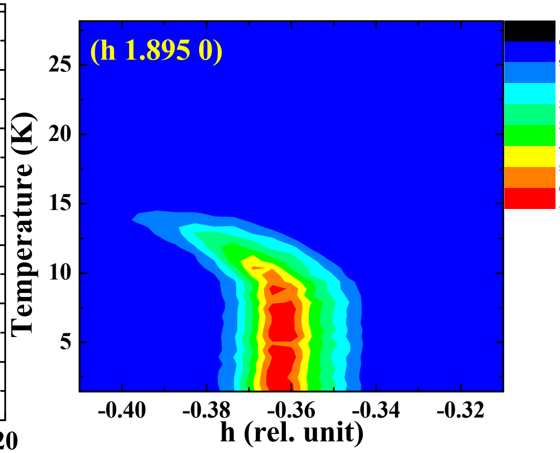

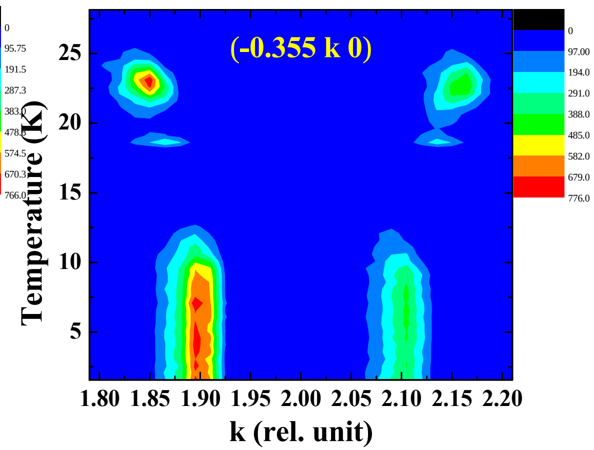

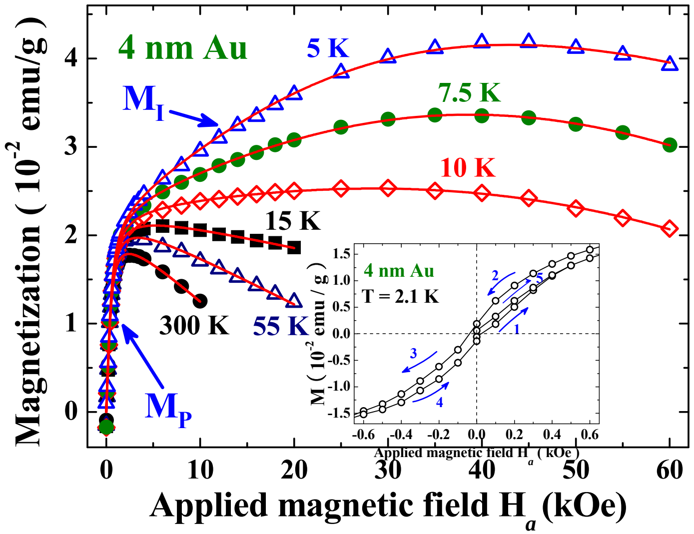

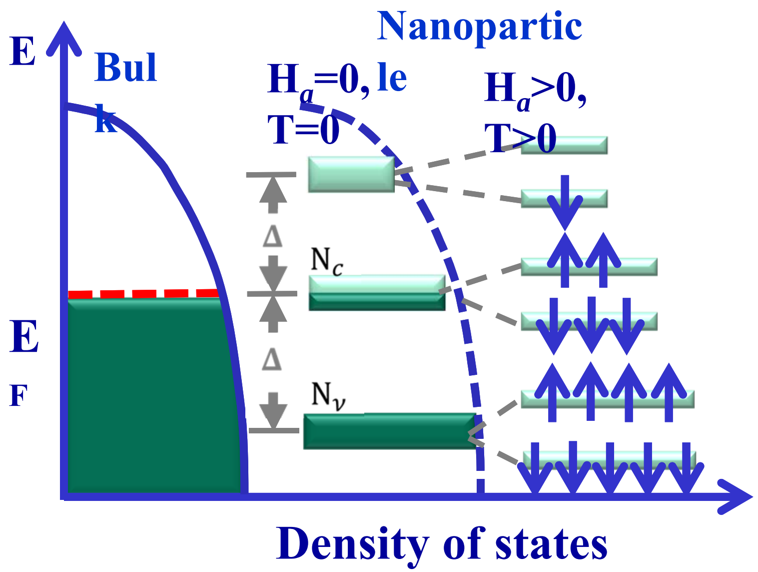

數據繪製與分析工具

Data Analysis and Graphing Software

Origin 7.5/8.0/8.5/9.0

- 匯入數據資料
- 多功能繪圖
- 數據分析與處理
- 可匯出多種檔案格式

www.originlab.com

海報與說明書製作
(尋找奇異、實作引導)

whli@phy.ncu.edu.tw

常見缺失

- 主題不明確：彈性力學、光電性質、
  -- 小而美、捨籠統、捨贅字
- 宣示性文辭：未考慮其他影響、能有效的、推翻
  -- 精準陳述、定性描述、定量證據
- 實驗環境不精準：紅濾光片、實驗室溫度
  -- 儀器解析度、參數可控、參數簡化
- 內容繁雜：第一代～第三代、實驗一～實驗十
  -- 捨棄測試、精挑新穎、化繁為簡
- 結論瑣碎：結論一～結論十五
  -- 陳述新穎、陳述新知、簡捷精準

展品内容

- 題目：具吸引力
- 摘要：要簡潔
- 主題：需引導
- 條文：要具體
- 結果：要顯眼
- 章節：獨立清晰
- 文辭：方便快速閱讀

海報主軸功效

重新整理作品的諸多結果，

理出清晰精要的結論，

以最具說服力的文字及圖示，

為作品爭得認同與最大的回響。

- 在有限的空間與時間，做最有效率的表達。
- 搭配視覺效果，組織清晰文字，介紹新穎。

展品海報編撰

彙整成果內容 -- 在於完整

評估成果內容 -- 在於精準

精選成果內容 -- 在於捨得

建構海報內容 -- 在於清晰

設計海報邏輯 -- 在於循序

編撰解說故事 -- 在於生動

境界:內容誠真、邏輯順善、版面精美

評審指標項目

- 創造能力 (creative ability)
- 科學思考 (scientific thought)
  工程目標 (engineering goals)
- 完整程度 (thoroughness)
- 研究技能 (skill)
- 瞭解程度 (clarity)
- 團隊合作 (team work)

展品內容

成果分享　　**簡潔、易讀、易懂**

題目：以一句文辭引起好奇、以一句文辭吸引眼光

摘要：以150字描述新穎發現(所作之事、所得結論)

背景知識：為何需要作本研究(已知與未知)

方法技術：材料系統、實驗裝置(架構、功能)、
實驗參數、實驗環境

成果內容：展現數據(順著邏輯循序介紹)
→ 看圖說話(用簡單規律描述)
→ 切入新穎(尋找奇異點)
→ 探討緣由(論述可能性)

結論：深遠意義、重要因子、新穎發現、指標影響

實例欣賞

(客觀心境、將心比心)

whli@phy.ncu.edu.tw

精選旅程

- 精挑耳目之利（選擇有力儀器）

  → 知己也知彼

（以拉橡皮筋實驗為例:皮膚感溫與真空中拉伸）

- 傾聽自然之聲（善選實驗參數）

  → 忘了我是誰

（以光槓桿振盪實驗為例:原理功能與非線性彈力）

（以線光束偏折實驗為例:數學推導與動態擴散）

精選旅程

- 尋找簡單之美（鑑定公因之術）

  → 慧眼識英雄

（以響片翻轉實驗為例:合力分析與旋轉態轉換）

（以水滴爬坡實驗為例:合力分析與渦流互勁）

- 訴說自然之音（精挑實驗成果）

  → 化繁為簡潔

（以奈米超導鐵硒實驗為例:苦工流程與精簡證據）

（以水滴在熱板上跳動實驗為例:以對稱性歸納）

國外得獎作品欣賞

Building bridges with water: the floating water birdge (2012, Intel 2nd Award)

- 在兩燒杯間建立水橋或液體橋
- 兩相互接觸燒杯、 內置去離子水、兩Pt電極、加dc 25 kV
- 慢慢拉離兩燒杯 → 水橋形成、可長至2.5 cm、可穩定至數小時
- 橄欖油/蓖麻油/甘油亦可，但橋較短
- 量測到電流、質量流、熱流 (IR相機)、燒杯間力 、液體溫度升高
- Due to the alignment of electrical dipole moments by dc voltage.

國外得獎作品欣賞

Carbon nanostructures via dry ice exposed to high temperature (2012, Intel 3rd Award)

- 主題：是否可以不透過化學反應製作工業用量碳奈米結構
- 方法：將乾冰置於高溫，3100 ^oC
- 高溫源：電銲
- 流程：以carbon arc furnace電銲乾冰，收集所有產品
- 電鍍成品：出現碳奈米管、碳奈米球、graphene
- 放置乾冰在carbon arc furnace兩電極間電銲時，碳奈米結構的平均產量為不放置乾冰時的16倍
- 結論：可行，可以不透過化學反應生產碳奈米結構
- 作品沒有分離所生產的各類碳奈米結構

題目實例比較

- 自製電磁力振盪器探討斑馬魚卵結構生物力學特性

  An investigation on the mechanics of Zebrafish eggs and their biological features with a uniquely-designed magnetic oscillator

- 以非線性震盪探討細胞彈性

  Studies of cell elasticity by nonlinear damping

- 水滴在高溫鋸齒上爬坡之物理機制探討
- 以溫差抗拒重力
- Climbing against gravity
- 幾何對稱破壞所引發的自發能源
- Self-propelled energy resource from geometrical symmetry breaking

題目實例比較

- 乒乓球彈跳運動研究
- 以電點接觸探討非線性形變

- 自製電磁力振盪器探討斑馬魚卵結構生物力學特性
- 以非線性震盪探討細胞彈性

- 水滴在高溫鋸齒上爬坡之物理機制探討
- 以溫差抗拒重力
- 幾何對稱破壞所引發的自發能源

- 鄒族之風聲-風笛
- 空氣訊息傳遞者

實例比較

- 主軸內容
- 捨棄繁贅
- 精挑議題
- 精選解說
- 引入狀況
- 解說方法
- 解說工具
- 解說參數
- 解說分析

Introduction

The compartments of cell organization can frequently be associated with their adhesive and elastic properties [1, 2]. To study elasticity of the membrane and viscosity of the cytoplasm in various stages of embryonic development [3], we constructed an electromagnetic oscillator [4] coupled to an optical lever to enhance the viscoelastic responses (Fig.1.b.). This device allows us to extract the elasticity coefficient and viscous damping coefficient of the cells in various stages of embryonic development, through nonlinear damping processes.

Materials and methods

1. Apparatus

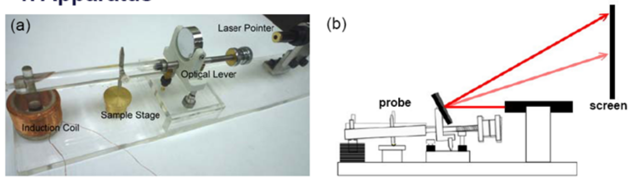

Fig.1. (a) Photo image and (b) schematic plot of the home-made electromagnetic oscillator.

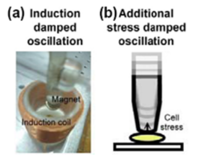

Fig.2. Schematic plot of the (a) induction damping and (b) additional stress damping.

- Force on sample can be adjusted by the current through the induction coil. (Fig.2.a.)
- Sample deformation is largely amplified by the optical lever.
- Sensitivity on deformation is between 0.5 μm and 2.5 mm.
- Forces on probe: electromagnetic induction, gravity, cell stress ,and cell adhesion
- Measurement: cell elasticity and cell adhesion

2. Physical parameters

Equation of motion:

$$M\ddot{X} = -kX - b\dot{X} + f_c(t, \Delta d)$$

- f_c: forces from the cell
- Δd: cell deformation

$$X(t) = A\exp(-\alpha t^{\beta})\sin(\omega t + \phi)$$

- A: amplitude of the oscillation
- ϕ: phase constant
- $\omega=(k/M)^{1/2}$: angular frequency, reflecting the elasticity of the cell
- $\alpha=b/2M$: damping constant, reflecting the status of internal structure
- β : dimensionless temporal exponent, reflecting the surface condition of the cell (Fig.3.)

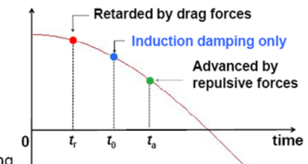

$t_r < t_0 \Rightarrow t_r = t_0^{\beta}$ with $\beta<1$

$t_a > t_0 \Rightarrow t_a = t_0^{\beta}$ with $\beta>1$

Fig.3. Physical meaning of nonlinear temporal exponent.

3. Stages of embryonic development of zebrafish

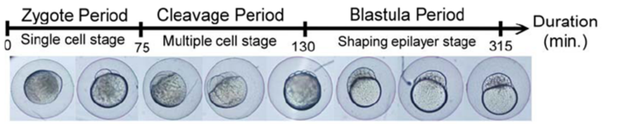

Fig.4. Development stages of zebrafish (*Danio rerio*) embryo.

實例比較

一維電磁孤立子(soliton)

(理論模擬研究)

- 孤立子： well-defined mass or charge or energy
- 僅繪製結論:難以理解
- 解說起始密度分布、電荷密度隨時間演進、起始密度較高之效應。

適當說明是必要的

引導進入狀況是必要的

Results only

2.Nonlinear effect:

(1) Electrostatic soliton:

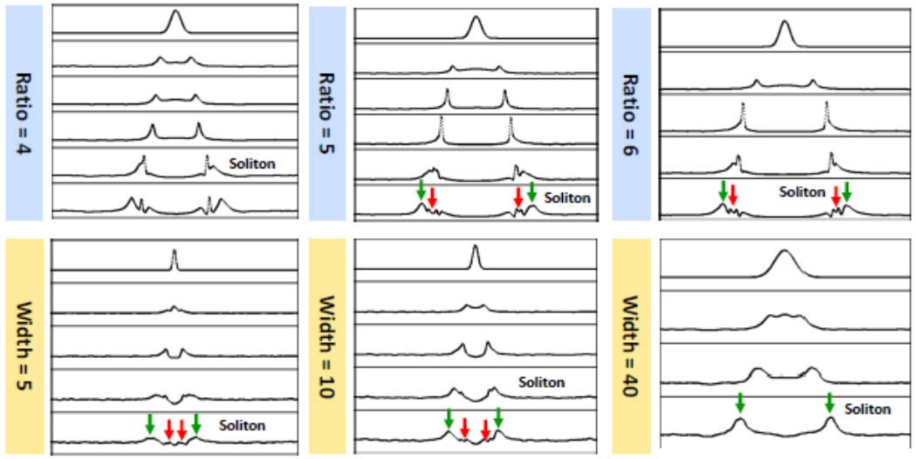

Nonlinear effect:

Excite the system by a pulse that carries a Gaussian charge package. The pulse has a higher density than the background density

With logic

(1)Electrostatic soliton:

R ≡ relative height of the pulse to the background.

W ≡ HWHM of the initial pulse.

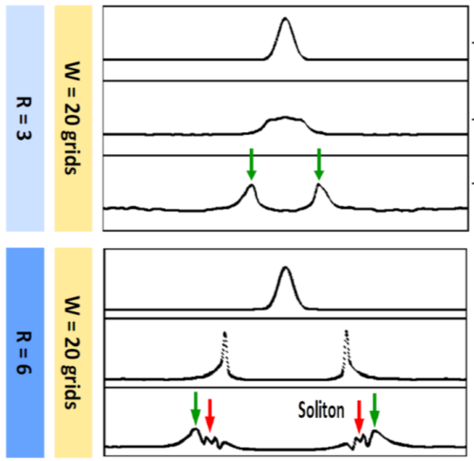

→ t= 0 sec Initial pulse.

→ t=100 sec The pulse spreads out.

→ t=200 sec Two solitons traveling in opposite directions are clearly visible.

- At R=6, the two solitons generated from the pulse continue to spread into more solitons.
- At R=6, the initial pulse carries more energy than the R=3 case. The speed of the solitons generated at R=6 is 2 times faster than which generated at R=3.

作品欣賞之1

Studies of cell elasticity by nonlinear damping (2011, Intel 2nd Award)

- 自製簡易磁動力光槓桿，記錄振盪曲線
- 光槓桿(放大微小型變)、磁動力(以磁力大小調變應力)
- 探針下放置軟物質，如斑馬魚卵，記錄光槓桿振盪曲線
- 如何理解振盪曲線所隱含的物理資訊
- 探針下壓：魚卵被壓縮，探討魚卵的抗拒能力(內部結構)
- 探針離開：魚卵黏滯探針，探討魚卵的黏滯力(表面特質)
- 探討孵化各週期、或各選定酸鹼環境下魚卵的彈力特質
- 需能描述非線性運動振盪
- 探針下壓時魚卵會滋生抗拒力保護自己

作品之精彩

以自製電磁力光槓桿探討軟物質：

- 自製簡易儀器可愛，
- 放大訊號讓儀器可用，
- 轉換各孵化期的組態數據成相關物理量，
- 量化黏滯彈性來討論各孵化期魚卵結構
  的改變。

展品欣賞

自製電磁力振盪器探討斑馬魚卵結構生物力學特性

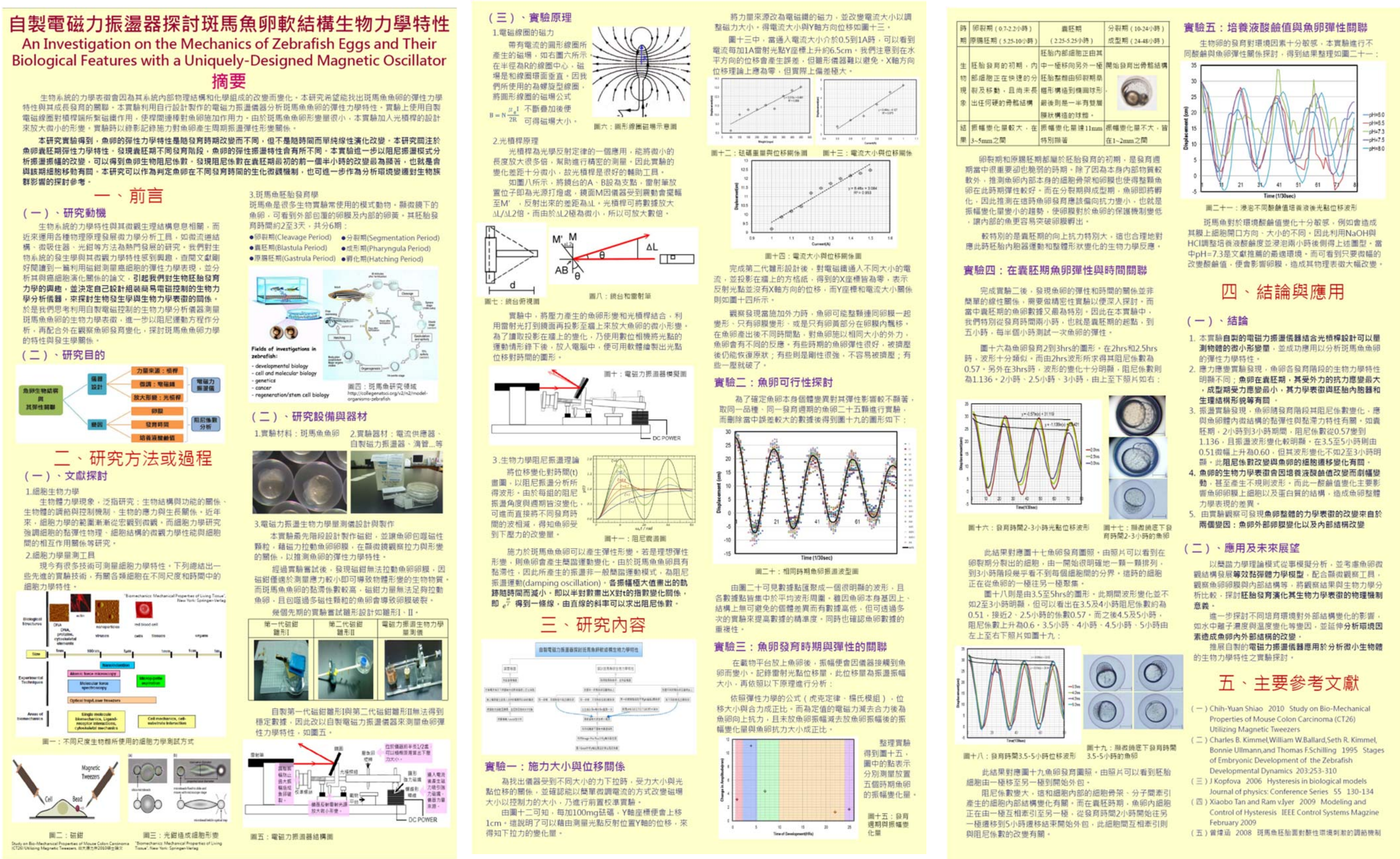

展品欣賞

Studies of cell elasticity by nonlinear damping

Introduction

The compartments of cell organization can frequently be associated with their adhesive and elastic properties [1, 2]. To study elasticity of the membrane and viscosity of the cytoplasm in various stages of embryonic development [3], we constructed an electromagnetic oscillator [4] coupled to an optical lever to enhance the viscoelastic responses (Fig.1.b.). This device allows us to extract the elasticity coefficient and viscous damping coefficient of the cells in various stages of embryonic development, through nonlinear damping processes.

Materials and methods

1. Apparatus

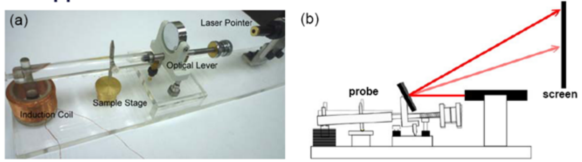

Fig.1. (a) Photo image and (b) schematic plot of the home-made electromagnetic oscillator.

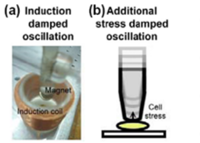

Fig.2. Schematic plot of the (a) induction damping and (b) additional stress damping.

- Force on sample can be adjusted by the current through the induction coil. (Fig.2.a.)
- Sample deformation is largely amplified by the optical lever.
- Sensitivity on deformation is between 0.5 μm and 2.5 mm.
- Forces on probe: electromagnetic induction, gravity, cell stress ,and cell adhesion
- Measurement: cell elasticity and cell adhesion

2. Physical parameters

Equation of motion:

$$M\ddot{X} = -kX - b\dot{X} + f_c(t, \Delta d)$$

- f_c: forces from the cell
- Δd: cell deformation

$$X(t) = A\exp(-\alpha t^{\beta})\sin(\omega t + \phi)$$

- A: amplitude of the oscillation
- ϕ: phase constant
- $\omega=(k/M)^{1/2}$: angular frequency, reflecting the elasticity of the cell
- α=b/2M : damping constant, reflecting the status of internal structure
- β : dimensionless temporal exponent, reflecting the surface condition of the cell (Fig.3.)

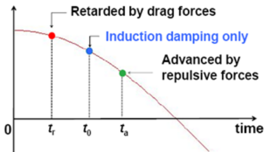

$t_r < t_0 \Rightarrow t_r = t_0^{\beta}$ with $\beta<1$

$t_a > t_0 \Rightarrow t_a = t_0^{\beta}$ with $\beta>1$

Fig.3. Physical meaning of nonlinear temporal exponent.

3. Stages of embryonic development of zebrafish

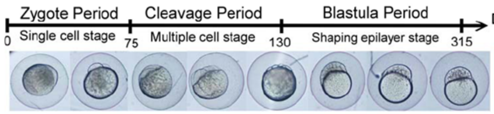

Fig.4. Development stages of zebrafish (*Danio rerio*) embryo.

Results and Discussion

Physical Analysis

1. Oscillation curve

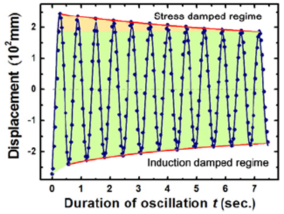

- Two regimes must be distinguished: An induction damped regime at the lower portion and a stress damped regime at the top.
- The damping oscillation can be described by forced oscillation but requires an exponent β for the temporal parameter in each regime.

Fig.5. A typical oscillation curve of the optical lever.

2. Nonlinearity

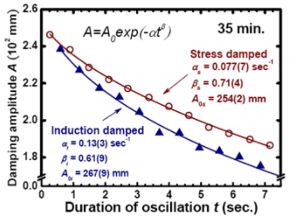

- α and β can be used to identify the cell stress and adhesion.
- $\alpha_s < \alpha_i$ indicates the stress force from the cell against the motion of the probe.
- $\beta_s > \beta_i$ shows that the adhesive force from the cell is working against the damping force from the electromagnetic induction.

Fig.6. Direct comparisons of the damping amplitudes observed in the two regimes

Applications

1. Mechanical hysteresis

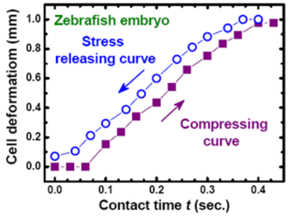

- Interestingly, mechanical hysteresis in the cell compressing and pressure releasing routes is clearly observed.
- The appearance of mechanical hysteresis reflects the existence of adhesive forces from the cell to the probe. It's magnitude can be identified from the enclosed area of the curve.

Fig.7. Mechanical hysteresis curve observed in the shaping epilayer stage.

2. Cell stress

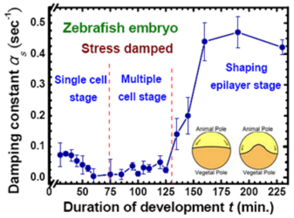

- In the single cell stage, the damping constant weakens in the course of development, reflecting that the movement of cytoplasm toward the animal pole will increase the elasticity of the cell.
- The cell elasticity remains essentially unchanged in the cell dividing period.
- The dramatic increase in the damping constant of the shaping epilayer stage echoes the building-up of local mass in the cell during this period.

Fig.8. Variations of the damping constant in the cell developing period.

3. Self protection

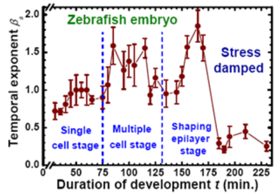

Fig.9. Variations of the temporal parameter in the developing periods.

- In the single cell stage, β gradually increases to reach unity. The retarded drag forces weakening in this period.
- In the cell dividing stage, β increases further to become repulsive (β >1).
- Interestingly, self-protection responses are observed, as the cell generates a resistive reaction to the external pressure.

4. Effects of pH pollution

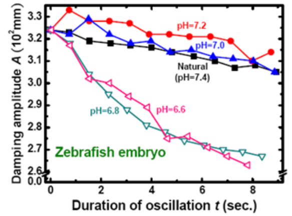

Fig.10. Damping amplitudes taken on the embryos developing in various acidic solutions.

- The oscillation profile is significantly altered, if the embryo is developed in a solution with a pH value smaller than 6.8 (0.2M NaH_2PO_4-Na_2HPO_4 Buffer).
- Developing the embryo in an acidic solution results in increases in the retarded drag forces from the embryo.
- Apparently, H^+/H_3O^+ ions can open up channels on the outer shell of the cell, which allow ions to diffuse into or out of the interior.

Conclusions

1. Cell elasticity and adhesion of zebrafish embryo have been measured using a home-made electromagnetic oscillator. Damping constant α, temporal exponent β, and angular frequency ω can be used to study the deforming force, adhesion, and elasticity of the cell.
2. The existence of cell adhesion is clearly demonstrated as the mechanical hysteresis curves appear in the damping routes.
3. Self-protection of zebrafish embryo is observed, as it generates resistive reactions to the external pressure throughout the development.
4. A slight change in the pH environment can significantly affect the embryo development.

References

[1] M. Krieg, Ph.D. thesis (Technische Universität, Dresden, 2009).

[2] P.-H. Puech, A. Taubenberger, F. Ulrich, M. Krieg, D. J. Muller, and C.-P. Heisenberg, J. Cell Science **118**, 4199 (2005).

[3] C. B. Kimmel, W. W. Ballard, S. R. Kimmel, B. Ullmann, and T. F. Schilling, Dev. Dyn. 203(3), 253 (1995).

[4] B. Ilic, Y. Yang, K. Aublin, R Reichenbach, S. Krylov, and H. G. Craighead, Nano Lett. **5**, 925 (2005).

Photos taken by authors

作品欣賞之2

Evuvuv – the air messager
(2007, Intel 2nd Award)

- 繩子拉接響片，接轉動馬達定速旋轉，記錄其運動軌跡
- 繩子：可扭轉、不可扭轉。
- 響片：薄片、圓柱、半圓柱、三角柱、四方柱
- 僅薄片接於可扭轉繩子，才能發出聲響
- 響片在衹角與仰角間連續轉換，響聲頻率也隨之改變
- 觀測到三旋轉態：繩子順時針方向扭轉、不扭轉、逆時針方向扭轉
- 聲音來源：spinning Evuvuv beating the air

展品欣賞

Euvuvu - the air messager

Introduction

An Euvuvu, a bamboo blade connected to a string, was once used for message delivery by ancient Tsou aborigines in Ali Mountain, Taiwan. It is nowadays still used to announce the opening of the Fona Festival, the most important annual event of Tsou aborigines. Fascinated by the sound produced by the Euvuvu, I then go through a series of studies to find the physics behind.

Materials and Methods

Setup

Figure 1 displays the components of the apparatus used in this study.

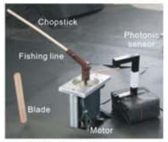

Fig. 1. Photo of the apparatus used in this study.

1. String connected to a chopstick, which serves as a fixed pivot point for rotation.
2. Decibel meter (Lutron SL-4001).
3. Voice recorder (CREATIVE MuVo TX FM).
4. Digital video camera (JVC GR-D93U).
5. Photoelectric counter (UPM-MF 2).
6. Laptop, equipped with Cool Edit 2000.

Operation

The Euvuvu is driven by a motor (Fig. 2) and the sound produced by an Euvuvu is recorded with a voice recorder (Fig. 3).

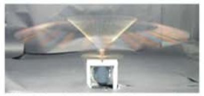

Fig. 2. An Euvuvu in rotation.

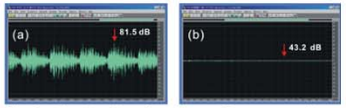

Fig. 3. (a) Sound produced by an Euvuvu, revealing a periodic nature in the sound frequency. (b) Sound produced by the background.

Parameters

1. Motor rotational speed (3.4 ~ 6.0 rps)
2. Shape of Euvuvu (blade, hemi-cylinder, cylinder, rectangular bar, triangular bar) (Fig. 4)
3. String type (twistable, untwistable)
4. Length of string (20 ~ 50 cm)
5. Diameter of string (0.313 ~ 0.533 mm)

Fig. 4. Shapes of the Euvuvu used in this study.

Results

Sound producers

The rotational modes and the capability in sound production of various Euvuvus are listed below.

Shape of blade \ Type of string	Twistable: Nylon	Twistable: Elastic string	Twistable: Cotton	Untwistable: Rotatable chain	Untwistable: Copper
(blade)	Revolution + spinning, sounding, automatic transition			Revolution + spinning, sounding, no transition	Revolution, no sound, no transition
(other shapes)	Revolution, no sound, no transition			Revolution, no sound, no transition	Revolution, no sound, no transition

▶ Only those Euvuvus that spin during revolution produce sound.

Rotational modes

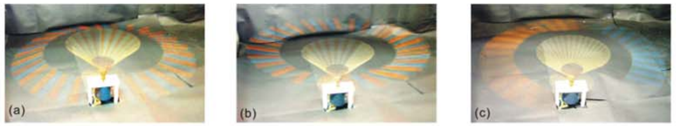

Fig. 5. Three rotational modes (a), (b), and (c) observed on the Euvuvu consists of a blade connected to a soft twistable string. (d) Sound produced by automatic transitions between modes (a) and (b) through mode (c). (e) No detectable sound is found in the mode (c).

During clockwise revolution, **clockwise** spinning of the blade results in revolution at an altitude **lower** than the pivot point [Fig.5(a)], while **counterclockwise** spinning gives a revolution **above** the pivot point [Fig.5(b)]. A periodic variation in sound frequency is observed in association with the spinning of the blade [Fig.5(d)]. A mode where the blade is not spinning [Fig.5(c)] is also found. It revolves at an **intermediate** altitude and produces no detectable sound [Fig.5(e)]. The rotational modes are summarized in Fig. 6.

A spin triplet state is observed (S=1)

Spinning	Clockwise	No spinning	Counter clockwise
Revolution	Below pivot point	Around pivot point	Above pivot point
Spinning mode (m_s)	-1	0	1
Sound	Yes	No	Yes

Fig. 6. Characteristics of the three spinning modes.

▶ The higher the revolution speed is, the louder the sound becomes. The longer the string is, the louder the sound becomes.

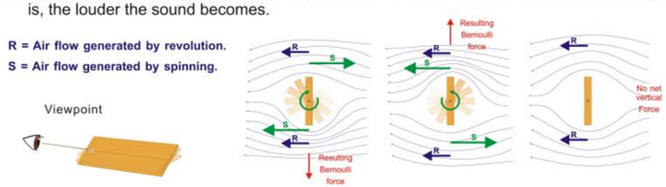

Fig. 7. Illustration of the forces that give rise to the three revolution modes, when viewed from the pivot point.

▶ It is the flows of the air near the edges of the Euvuvu that define the resulting vertical force. A downward, an upward, and no net vertical Bernoulli forces may be created, that in turn produce the three possible revolution modes, as shown in Fig. 7.

Transition between modes

▶ The appearance of a periodic variation in the sound frequency shows that the spinning rate of the Euvuvu varies periodically, as shown in Fig. 8.

▶ The frequency of the sound produced is found to be exactly twice the spinning rate of the Euvuvu, as can be seen in Fig. 8. This indicates that the sound produced is directly associated with the spinning of the Euvuvu, rather than with its revolution.

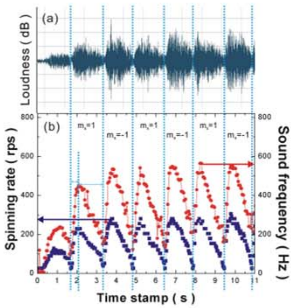

Fig. 8. (a) Sound wave produced by a bamboo blade connected to a fishing line. (b) A direct comparison between the spinning rate of the Euvuvu and the frequency of the sound it produces.

▶ The progressive decrease in the spinning rate simply reflects the twist torque gradually accumulated in the string.

▶ Whenever a string that can preserve twist torque is used, automatic transition between the spinning modes becomes feasible.

▶ No variation in the sound frequency is found in the Euvuvu connected to a untwistable string.

Lifetime of rotational modes

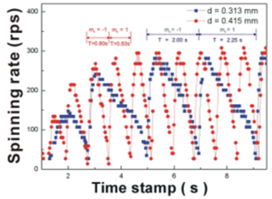

Fig. 9. The effect of string diameter on the spinning rate of the Euvuvu.

A shorter lifetime of revolution is observed when a twistable string of a larger diameter is used, as can be seen in Fig. 9. This is consistent with the fact that a string of a larger diameter is harder to twist.

Both the lifetimes of the $m_s = 1$ and that of -1 modes are found to vary with the string diameter as $T \propto d^{-n}$ with $n \approx 3$, as shown in Fig. 10. This shows that the energy needed to twist the string is proportional to d^3. It is this energy stored in the string that initiates the automatic transition between rotational modes.

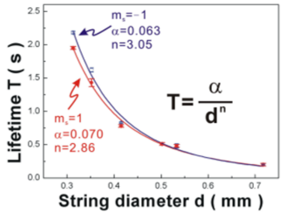

Fig. 10. Variations of the lifetimes of the rotational modes with string diameter.

A d^4-dependency of the twist torque on string diameter is expected for static twisting. The d^3-dependency observed in the Euvuvu signals that it is the dynamic twisting which governs the energy transfer rate between the blade and the string.

No obvious energy dissipation to the string is found in the time period studied.

Conclusions

1. The sound produced by the Euvuvu is a direct result of the spinning Euvuvu beating the air. An unspinnable Euvuvu produces no sound.
2. The rotational modes associated with an Euvuvu are in fact controlled by the spinning of the Euvuvu.
3. Three rotational modes are found. Automatic transition between the modes can be created by using a twistable string that serves to store and release the spinning energy.
4. In ancient times, the Euvuvu was used by the Tsou aborigines as a tool for message delivery. Thus, it is important to maximize its loudness. A long flat piece of bamboo connected to a twistable string makes a perfect Euvuvu for message delivery. I admire the aborigines' scientific wisdom.

References

1. T. Pima, *Tsou Aborigines in Taiwan*, p.273, (TaiYuan Press, Taipei, 2003).
2. P. G. Hewitt, *Conceptual Physics: With Expanded Technology : The High School Physics Program*, chap. 9, (Addison-Wesley Pub, 3rd ed. 1999).
3. J. E. Allen, *Aerodynamics*, (Granada Press, London, 1982).
4. http://www.wordpedia.com/search/Content.asp?ID=44603

All the photos are taken by the author.

作品欣賞之3

Nonlinear diffusion dynamics measured by simple light-transmission method
(2010, Intel 3rd Award)

- 雷射筆光點通過玻璃棒 → 單色光線光源
- 一液體懸浮在另一液體上方 → 介面間兩液體相互擴散
- 單色光線光源通過介面區域，偵測透射光形狀，記錄透射光形狀隨時間的變化
- 光透射過介面被曲折的程度與介面的密度有關 → 推算出介面區域密度隨時間的改變量
- 量測出一液體擴散至另一液體的位能障值
- 303 K的熱能就能有效的破壞甘油間分子間的鍵能
- 甘油-水介面：初期，水與甘油間形成氫鍵引發擴散
  後期，水與甘油間密度的不同引發擴散

作品之精彩

以簡單的光穿透量測非線性擴散動力學

- 液體介面的動態擴散
- 以簡單的折射定律判定混合液體之密度
- 能量測擴散過程的動態行為
- 實驗技術應用在甘油與水的介面系統
- 觀測到初期的擴散主控於水與甘油間形成氫鍵所引發。

展品欣賞

簡易方法量測擴散係數

Nonlinear diffusion dynamics measured using a simple light-transmission method

INTRODUCTION

Refractive index of a liquid depends strongly on the concentration of the solution. It is known that a concentration gradient will be generated in the interface regime when two different liquids are brought in contact. When a line laser beam is directed onto the interface of the two different liquids, it will produce a Gaussian line upon transmission [1]. The transmitted Gaussian profile is very sensitive to the concentration gradient in the interface regime [2]. We set up a simple apparatus which is able to measure this transmitted profile timely. By measuring the time evolution of such transmitted Gaussian profiles [3], the diffusion dynamics between two different liquids can then be revealed.

MATERIALS AND METHODS

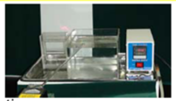

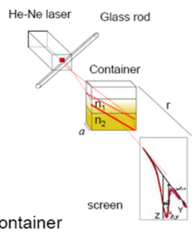

Fig. 1 Schematic of the experimental setup

- Physical parameters :
  - C : weight concentration
  - n : refractive index of the liquid
  - D : diffusion coefficient
  - t : duration time
  - T : temperature
  - a : the width of the container
  - r : the distance between the screen and container
  - y : the shift of the dip along reference line
  - z : the vertical shift of the dip

- Assuming the diffusion coefficient is independent of concentration of the solution, the Fick's law gives

$$\frac{dC}{dy} = \frac{n_1 - n_2}{2\sqrt{\pi D t}} \exp\left(-\frac{y^2}{4Dt}\right)$$

- 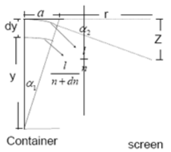

$$\Rightarrow \frac{dn}{dy} = \frac{Z}{ar}$$

l : optical path
α_1 : $\tan^{-1}$ (a/y)
α_2 : the refractive angle

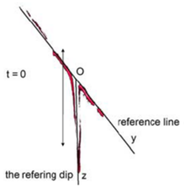

Before diffuse t = 0 t = 4,020 t = 9,060 sec

Fig. 2 Time evolution of the transmitted laser line profile.

The transmitted line profiles taken at a specific time reflect the inter diffusion behavior at that time.

RESULTS AND DISCUSSION

The phenomenon of diffusion

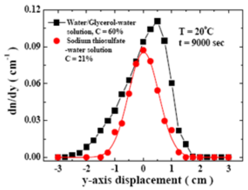

Fig. 3 Direct comparison of dy/dn along the y-axis direction for water to diffuse into the two solutions.

- The asymmetric profile of the dy/dn line observed for the water/glycerol-water solution (Fig. 3, filled squares) showing that the diffusion in such a system occurs in both directions, where water and glycerol molecules can effectively diffuse into each other.
- The symmetric profile of the dy/dn line observed for the water/sodium thiosulfate-water solution (Fig. 3, filled circles) reflecting that the diffusion occurs only around the interface regime.

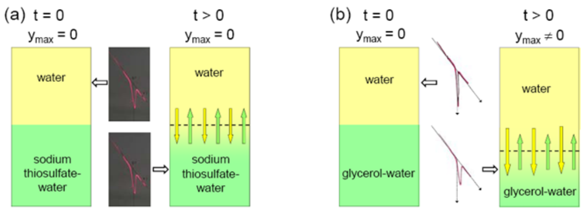

Fig. 4 Schematic illustrations of diffusion dynamics of (a) Sodium thiosulfate-water solution. (b) Glycerol-water solution, where y_{max} indicates the postion of the maximum of dn/dy along y-axis.

Potential barrier for diffusion

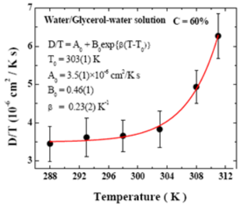

Fig. 5 Temperature dependence of the diffusion coefficient of water/glycerol-water solution.

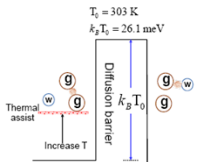

Fig. 6 Schematic illustration of the potential barrier for forming water-glycerol complex.

- The thermal diffusion coefficient of the glycerol-water solution exhibits a sharp increase above 303 K (Fig 5), which can be described using an exponential increasing function (solid line).
- The changes can be originated from the breaking of glycerol-glycerol bond, which allows the formation of hydrogen bonds between water and glycerol molecules to form water-glycerol complexes.
- The temperature constant T_0 = 303 K obtained from the fit represents the temperature above which the thermal energy can effectively break the glycerol-glycerol complex to form water-glycerol complexes. (Fig. 6).
- The D/T of water/sodium thiosulfate-water solution exhibits a linear increase with increasing temperature, showing that there is no critical potential barrier for the diffusion in the room temperature regime. This character of D/T may reflect the diffusion to occur mainly in the interface region.

Diffusion dynamics during diffusion

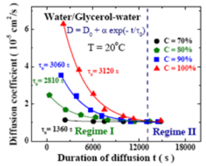

Fig. 7 Variations of diffusion coefficient of water/glycerol-water solution with duration of diffusion.

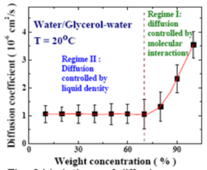

Fig. 8 Variations of diffusion coefficient of water/glycerol-water solution with weight concentration.

- The higher diffusion coefficient for the solution with a higher glycerol concentration reflects that the interaction between glycerol and water molecules is noticeably stronger than that among glycerol molecules.
- The amount of water diffuses into the glycerol-water solution decays exponentially with duration of diffusion but reduces to a finite value (Fig 7), showing that there are two mechanisms that control the diffusion.
- Interestingly, the diffusion coefficients of all solutions reduce to the value of the C=70% solution.
- The diffusion coefficient exhibits a sharp increase as the glycerol weight concentration is higher than 70%, at which the molar ratio of glycerol/water is about 1/3 (Fig. 8).

The mechanism behind the diffusion

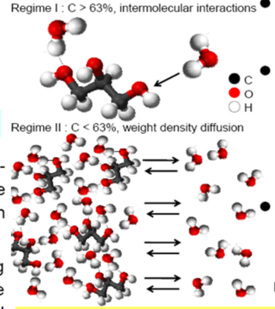

- There are three OH groups available for inter molecular bonding in each glycerol molecule.
- Regime I : Diffusion controlled by inter-molecule interactions. In the present case, it is the formation of hydrogen bonds between glycerol and water molecules that trigger the diffusion (Fig. 9).
- Regime II: Diffusion controlled by the similar but slight difference in water and glycerol densities.

Fig. 9 Schematic illustration of the two mechanisms

CONCLUSIONS

- We provide a simple setup and an easy method to quantitatively determine the variation in diffusion coefficient during the process, which can qualitatively reveal the diffusion barrier.
- A thermal energy higher than T_0=303 K can effectively break the bonding between glycerol-glycerol molecules.
- Two mechanisms that trigger the diffusion in glycerol-water solution have been identified. Inter-molecule interactions control the diffusion in high concentration, whereas the weight density differences between the liquids drive the diffusion when inter-molecule bonding have been saturated.

REFERENCES

1. A. J. Barnard and B. Ahlborn, Am. J. Phys. **43**(7), 573 (1975).
2. F. A. Bassi, G. Arcovito, and G. D'Abramo, J. Phys. E **10,** 249 (1977).
3. G. Gaffney and C.-K. Chau, Am. J. Phys. **69**, 821 (2001).

展品欣賞

Self-propelled Energy Resource from Geometrical Symmetry Breaking

Introduction

It is known that a liquid droplet can stand on an extremely hot plate for a long period of time, by means of the formation of an insulating vapor layer underneath. This vapor layer limits heat transfer between the droplet and the hot plate [1, 2]. A self-propelled engine that consumes the atomic binding energy can be manufactured by breaking the geometrical symmetry of the droplet. This self-propelled engine is demonstrated by setting the droplet to climb against gravity on an asymmetrical saw-tooth surface. The self-propelled machinery can also be triggered by edges to generate damped oscillations of the droplet on a hot smooth plate.

Materials and Methods

I The phenomena

1 Climbing against gravity

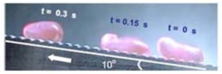

Fig. 1 Superimposed time-lapse photos of a droplet that is climbing against gravity

(1) A droplet at 25 °C can climb against gravity on a 10°-inclined saw blade at 300 °C (Fig. 1). The climbing speed can reach as high as 20 cm/s.

(2) Once the droplet reaches the unheated region of the plate, the droplet is rapidly evaporated.

2 Deformation and oscillation

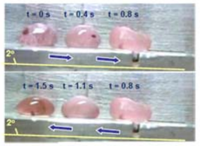
Fig. 2 Superimposed time-lapse photos of a droplet that is oscillating on a hot smooth surface

(1) An oscillator can be formed on an inclined smooth surface at 200 °C (Fig. 2).

(2) An edge on a hot smooth surface can reverse the sliding-down droplet to climb against gravity.

(3) The droplet oscillates back and forth at the expense of its own mass before reducing to a critical small size of ~ 4 μl.

II Critical parameters

1 Heat shielding

(1) The temperature of the plate is critical for the formation of a supporting vapor layer underneath. This layer protects the droplet from being violently evaporated (Fig. 3).

(2) A plate at 300 °C can generate a heat shielding vapor layer of 0.1 mm thick.

Fig. 3 Droplet-vapor profiles on a (a) 200 °C and (b) 300 °C hot saw- tooth surface

2 Uneven vortices

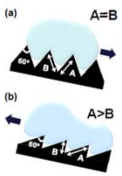

(1) A droplet on a symmetrical saw-tooth surface (Fig. 4a) slides down.

(2) A droplet on an asymmetrical saw-tooth surface (Fig. 4b) deforms into an uneven dumb bell shape of circulating liquid vortices and moves against the long segments of the saw teeth.

Fig. 4 Schematic drawings show the conformations of droplets on (a) symmetrical and (b) asymmetrical saw-tooth surfaces.

Results and Discussion

I Self-propelled engine

1 Dynamical vortices

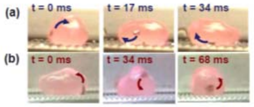

Fig. 5 Internal flows of (a) the large and (b) the small vortices of a droplet on a 2°- inclined saw tooth surface at 300 °C

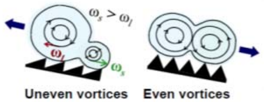

Fig. 6 Momentum generated by vortices that are circulating above various axes

(1) The liquids in the uneven dumb-bell shaped droplet are circulating separately about horizontal axes, but in opposite directions and at different speeds (Fig. 5). Average angular speeds found for the large and the small vortices are ω_l = 20.1 and ω_s = 22.5 π rad/s, respectively (Fig. 6).

(2) It is the evaporated liquid at the contact that drives the circulation of vortices above.

(3) The momentum difference generated between the large and the small vortices (Fig. 6) results in a driving momentum, which triggers the droplet as a whole to roll towards the large vortex side.

(4) Two vortices of similar sizes can not generate strong enough net driving momentum for rolling along a specific direction but moving around (Fig. 6).

2 Asymmetrical competition

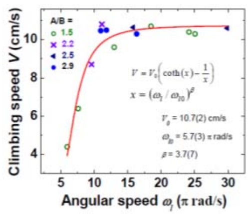

Fig. 7 Variations of the climbing speed with the angular speed of the large vortex, where different symbols indicate observations from various ratios of the two segments. The solid line indicates the Langevin profile obtained from data fitting.

(1) The climbing speed of the droplet is found to be saturated as the angular speed of the large vortex is increased further (Fig. 7).

(2) The saturation follows the Langevin profile, showing that the phenomenon can be described by a driving parameter ω_l from the large vortex and a dragging parameter ω_{l0} from the small vortex and friction.

3 Thermal perturbation

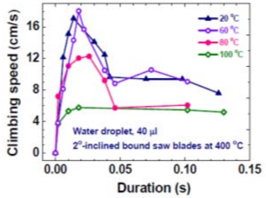

Fig. 8 Variations of the climbing speed of a water droplet with time at various temperatures

(1) The climbing reaches equilibrium at ~0.04 s. The climbing speed can reach as high as 18 cm/s, which is found to be significantly reduced, rather than increased, as the temperature of the droplet approaches the boiling point (Fig. 8).

(2) It is the boiling of the liquid that disturbs its circulation, which results in a reduction of the net driving momentum, hence the climbing capability.

(3) Significant reductions of the climbing speed appear before it stabilizes. This shows that the small vortex stabilizes after the large one.

II Damped bound state

1 Single trigger

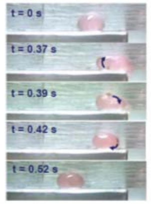

(1) A droplet sliding down on an inclined smooth surface can be bounced back to become climbing up by an edge on the surface. It oscillates back and forth on the surface (Fig. 9).

(2) The droplet deforms and evaporates, in some degree, once reaches the edge, which produces upward force to generate a clockwise vortex.

Fig. 9 A series of photos indicates a 30-μl droplet oscillating on an inclined smooth surface.

2 Double trigger

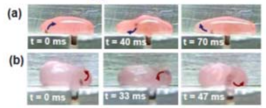

Fig. 10 Internal flows of (a) the large and (b) the small vortices of a droplet

(1) A droplet larger than 50 μl requires two edges to trigger a larger deformation for reversing its motion (Fig. 10).

(2) The vortices generated by the two edges are circulating along opposite directions (Fig. 10).

3 Energy resources

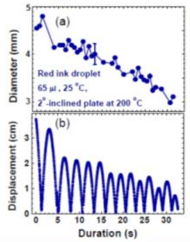

Fig. 11 (a) Diameter and (b) displacement of a droplet oscillating on a smooth surface

(1) The sizes of the climbing droplet as well as oscillating one are found to be gradually reduced upon rolling on the surface (Fig. 11a).

(2) The amplitude of the oscillation is also found to be reduced in association with the reduction of its own mass(Fig. 11). This behavior can be due to the reduction of the vortex sizes that limits the circulation and driving momentum.

Conclusions

1 A supporting vapor layer underneath the droplet can protect it from being violently evaporated for a self-propelled engine of droplets on a hot surface.

2 The key is to produce two uneven liquid vortices that are circulating about horizontal axes in opposite directions and at different speeds.

3 It's the atomic binding energy released from evaporation that provides the energy for vortex circulation and droplet motion.

4 Vortex instability from local turbulence can significantly reduce the self-propulsion capability.

Potential Application

Delivery of cold liquids into the remote or hard-to-reach cores of hot sources for temperature control or emergency cooling of the cores at specific spots.

References

[1] H. Linke, B. J. Aleman, L. D. Melling, M. J. Taormina, M. J. Francis, C. C. Dow-Hygelund, V. Narayanan, R. P. Taylor and A. Stout, Phys. Rev. Lett. **96**, 154502 (2006).

[2] Leidenfrost effect, Wikipedia, http://en.wikipedia.org/wiki/Leidenfrost_effect .

Photos taken by author

细火精燉

且看欲盡花經眼
莫厭傷多酒入唇
細推物理須行樂
何用浮榮絆此身

杜甫:曲江二首，唐(8世紀)

- 且看 → 欣賞自然、發現自然
- 莫厭 → 安心探索、欣賞迷茫
- 細推 → 深層探索、邏輯推演
- 行樂 → 抽絲頓悟、分享新穎
- 浮榮 → 自享成果、何樂評審